Expression and permeation properties of the K^+ channel Kir7.1 in the retinal pigment epithelium

Masahiko Shimura*, Yukun Yuan*, Jinghua T. Chang‡, Suiyuan Zhang‡, Peter A. Campochiaro‡§, Donald J. Zack‡§‖ and Bret A. Hughes*†

**W. K. Kellogg Eye Center, Department of Ophthalmology and Visual Sciences and †Department of Physiology, University of Michigan, Ann Arbor, MI and ‡Wilmer Eye Institute and Departments of §Neuroscience and ‖Molecular Biology and Genetics, Johns Hopkins University School of Medicine, Baltimore, MD, USA*

(Received 30 June 2000; accepted after revision 31 October 2000)

1. Bovine *Kir7.1* clones were obtained from a retinal pigment epithelium (RPE)-subtracted cDNA library. Human RPE cDNA library screening resulted in clones encoding full-length human *Kir7.1*.

2. Northern blot analysis indicated that bovine *Kir7.1* is highly expressed in the RPE.

3. Human Kir7.1 channels were expressed in *Xenopus* oocytes and studied using the two-electrode voltage-clamp technique.

4. The macroscopic Kir7.1 conductance exhibited mild inward rectification and an inverse dependence on extracellular K^+ concentration ($[K^+]_o$). The selectivity sequence based on permeability ratios was K^+ (1.0) ≈ Rb^+ (0.89) > Cs^+ (0.013) > Na^+ (0.003) ≈ Li^+ (0.001) and the sequence based on conductance ratios was Rb^+ (9.5) ≫ K^+ (1.0) > Na^+ (0.458) > Cs^+ (0.331) > Li^+ (0.139).

5. Non-stationary noise analysis of Rb^+ currents in cell-attached patches yielded a unitary conductance for Kir7.1 of ~2 pS.

6. In whole-cell recordings from freshly isolated bovine RPE cells, the predominant current was a mild inwardly rectifying K^+ current that exhibited an inverse dependence of conductance on $[K^+]_o$. The selectivity sequence based on permeability ratios was K^+ (1.0) ≈ Rb^+ (0.89) > Cs^+ (0.021) > Na^+ (0.003) ≈ Li^+ (0.002) and the sequence based on conductance ratios was Rb^+ (8.9) ≫ K^+ (1.0) > Na^+ (0.59) > Cs^+ (0.23) > Li^+ (0.08).

7. In cell-attached recordings with Rb^+ in the pipette, inwardly rectifying currents were observed in nine of 12 patches of RPE apical membrane but in only one of 13 basolateral membrane patches.

8. Non-stationary noise analysis of Rb^+ currents in cell-attached apical membrane patches yielded a unitary conductance for RPE Kir of ~2 pS.

9. On the basis of this molecular and electrophysiological evidence, we conclude that Kir7.1 channel subunits comprise the K^+ conductance of the RPE apical membrane.

The retinal pigment epithelium (RPE) is a simple cuboidal epithelium in the distal retina that separates the photoreceptor cells from their main blood supply in the choroid. From this strategic position, the RPE carries out a host of functions that are critical to the visual process. One of these is the transepithelial transport of fluid, ions and metabolites, which serves to control the composition and volume of the extracellular fluid that surrounds the photoreceptor outer segments (Hughes *et al.* 1998).

It is well established that K^+ channels play a central role in the vectorial transport of K^+ across the RPE. At the apical membrane, the net flux of K^+ into or out of the subretinal space is determined by the balance between K^+ efflux through Ba^{2+}-sensitive K^+ channels (Lasansky & De Fisch, 1966; Miller & Steinberg, 1977; Griff *et al.* 1985; Joseph & Miller, 1991; Quinn & Miller, 1992) and K^+ influx via the electrogenic Na^+–K^+ pump (Miller *et al.* 1978) and Na^+–K^+–$2Cl^-$ cotransporter (Miller & Edelman,

1990; Joseph & Miller, 1991). At light onset, a decrease in subretinal K^+ concentration, originating from a change in photoreceptor activity, causes an increase in the efflux of K^+ through the apical K^+ channels, leading to the reversal of net K^+ transport from absorption to secretion (Bialek & Miller, 1994).

In patch-clamp studies on RPE cells isolated from a variety of vertebrate species, we have shown that the predominant conductance in the physiological voltage range is an inwardly rectifying K^+ (Kir) conductance (Hughes & Steinberg, 1990; Hughes & Takahira, 1996, 1998). The inward rectification of this K^+ conductance is relatively weak, such that it supports substantial outward K^+ current at voltages positive to the K^+ equilibrium potential. This conductance has several remarkable properties, including an inverse dependence on extracellular K^+ concentration (Segawa & Hughes, 1994; Hughes & Takahira, 1996) and an intracellular Mg-ATP requirement for sustained activity (Hughes & Takahira, 1998). Blocker sensitivity studies on the intact RPE sheet preparation indicate that these Kir channels underlie that apical membrane K^+ conductance (Hughes *et al.* 1995*a*).

In the mid-1990s, expressional cloning of the inwardly rectifying K^+ channels ROMK1 (Ho *et al.* 1993), IRK1 (Kubo *et al.* 1993) and GIRK (Kofuji *et al.* 1995) established the existence of a new gene family distinct from the voltage-gated K^+ channel family. Since then, several other members of the Kir channel family have been identified, increasing the number of members to 15 (Reimann & Ashcroft, 1999). The most recent addition is Kir7.1, an inwardly rectifying K^+ channel with several novel properties, including a macroscopic conductance with low dependence on extracellular K^+ concentration ($[K^+]_o$) (Döring *et al.* 1998; Krapivinsky *et al.* 1998), a low unitary conductance estimated to be ~50 fS (Krapivinsky *et al.* 1998), and an unusually large Rb^+-to-K^+ conductance ratio (Wischmeyer *et al.* 2000). Kir7.1 expression has been reported in certain epithelia such as choroid plexus and small intestine, as well as in stomach, kidney, thyroid follicular cells, brain, spinal chord and testis (Döring *et al.* 1998; Krapivinsky *et al.* 1998; Partiseti *et al.* 1998; Nakamura *et al.* 1999, 2000). The capacity of this channel to pass large outward K^+ currents makes it well suited to function in epithelial ion transport processes (Döring *et al.* 1998).

In this study, we have cloned bovine Kir7.1 from a subtracted RPE cDNA library (Chang *et al.* 1997, 1999), obtained its human orthologue and confirmed its expression in the RPE by Northern blot analysis. Furthermore, we have compared the permeation properties of the native Kir channel in freshly dissociated bovine RPE cells to those of cloned Kir7.1 channels expressed in *Xenopus* oocytes and find that they are nearly identical. Some of these results have been published in abstract form (Shimura *et al.* 1999; Yuan *et al.* 2000).

METHODS

Isolation of human Kir7.1 cDNA

Over a thousand clones from a bovine RPE cDNA library that had been 'subtracted' with biotinylated heart and liver RNA were partially sequenced using a combination of manual and automated (Beckman CEQ2000) dideoxy sequencing (Chang *et al.* 1997, 1999). Using as a probe the insert of a clone having sequence homology to ROMK2, a human RPE cDNA library was screened. Resultant positive clones were plaque purified and sequenced. Methods used for library screening and other routine recombinant DNA analyses were essentially as described in standard laboratory manuals (Sambrook *et al.* 1989; Ausubel *et al.* 1996).

Northern analysis

For Northern analysis, an RNA blot was prepared by loading 10 μg total mRNA isolated from various bovine tissues. The blot was sequentially hybridized with a partial-length bovine Kir7.1 cDNA probe at 42 °C in 50 % formamide, 6 × SSPE (saline–sodium phosphate–EDTA buffer) and 0.5 % SDS. After 24 h of hybridization, membranes were washed twice at low stringency (42 °C, 2 × SSPE with 0.1 % SDS). Blots were then exposed to X-ray film for 24 h.

Expression of Kir7.1 in *Xenopus* oocytes

For the construction of a transcription plasmid, the coding region of human Kir7.1 cDNA (nucleotides 90–1303 of pc84 cDNA) was PCR amplified with the Expand High Fidelity PCR system (Boerhinger Meinheim, Indianapolis, IN, USA) and subcloned into the polyadenylating transcription vector pBSTA (Goldin, 1992) at the *Bgl*II site using a blunt end-ligation procedure. The resulting plasmid contained the cloned cDNA insert flanked by the 5′ and 3′ untranslated regions of the *Xenopus* β-globin gene and allowed sense-strand cDNA to be transcribed by T7 RNA polymerase. Capped poly(A)$^+$ RNA was synthesized from plasmid cDNA linearized at the *Sac*I site using a commercially available cRNA capping kit (Ambion Inc., Austin, TX, USA). cRNA was precipitated in 70 % ethanol and re-dissolved in diethyl pyrocarbonate (DEPC)-treated water.

All experiments with *Xenopus* frogs were carried out following protocols approved by the University of Michigan Committee on the Use and Care of Animals. *Xenopus laevis* oocytes were surgically removed from adult females anaesthetized with topical tricaine methane sulfonate (0.15 % for 15–30 min) and defolliculated by incubating clusters of oocytes in 0.2 % collagenase (type IV, Sigma Chemical Co., St Louis, MO, USA) in calcium-free ND96 solution (96 mM NaCl, 2 mM KCl, 1 mM $MgCl_2$, 10 mM Hepes (pH 7.4), 300 mg ml^{-1} gentamicin and 550 mg ml^{-1} sodium pyruvate). Incisions were sutured and frogs were allowed to recover with aftercare. Healthy stage V–VI oocytes were collected and stored overnight at 18 °C in ND96 solution plus 1 mM $CaCl_2$. Defolliculated oocytes were injected with 5–10 ng of Kir 7.1 cRNA in 50 nl and maintained at 18 °C in incubation solution for up to 72 h before recording. Oocytes injected with the same volume of DEPC-treated water served as controls.

Experiments on Kir7.1 cRNA-injected oocytes

Solutions. The standard bath solution for *Xenopus* oocyte recordings consisted of (mM): 96 NaCl, 2 KCl, 10 Na-Hepes, 1.0 $CaCl_2$, 1.0 $MgCl_2$, pH 7.4. To study the dependence of Kir7.1 currents on extracellular K^+, the concentration of K^+ ($[K^+]_o$) was varied by equimolar replacement with Na^+. In experiments investigating the permeability of Kir7.1 to monovalent cations, the solution consisted of (mM): 98 X, 10 NMDG-Hepes, 1.0 $CaCl_2$, and 1.0 $MgCl_2$, where X is KCl, NaCl, RbCl, LiCl, or CsCl. When indicated, 10 mM $BaCl_2$ was added directly to the external solution.

Electrophysiology. Whole-cell currents were recorded using the two-electrode voltage-clamp technique (Stuhmer, 1992). Microelectrodes, pulled from thick-wall borosilicate glass (o.d. = 1.0 mm, i.d. = 0.5 mm) with a multistage programmable puller (Sutter Instruments, San Rafael, CA, USA) and having an impedance of 0.5–1.5 MΩ when filled with 3 M KCl, were used as voltage-sensing and current-passing electrodes. Signals from the current-passing electrode were amplified using a GeneClamp 500 amplifier (Axon Instruments, Inc., Burlingame, CA, USA) with the built-in low pass filter set to 0.5–1 kHz and stored on a computer hard drive for later analysis. To avoid voltage errors due to large currents (Baumgartner *et al.* 1999), data from oocytes exhibiting currents $> 25\ \mu$A at −160 mV were rejected. Data acquisition and analysis were performed with pCLAMP 6.0 software (Axon Instruments, Foster City, CA, USA).

For cell-attached patch recordings, the vitelline membrane was manually removed after exposing oocytes to a hypertonic solution (400 mosmol (kg H_2O)$^{-1}$: 220 mM NMDG-Cl, 5 mM EGTA-KOH, 1 mM $MgCl_2$ 10 mM Hepes) for 5–10 min. Patch pipettes were pulled from 7052 glass tubing (o.d. = 1.65 mm, i.d. = 1.2 mm, Garner Glass, Claremont, CA, USA) and heat-polished to a resistance in the range 0.5–2 MΩ. Currents were recorded with an Axopatch 200 amplifier (Axon Instruments) with the built-in low pass filter set to 4 kHz.

Experiments on isolated bovine RPE cells

Cell isolation. Adult bovine eyes were obtained from a local abattoir within 30 min of death and placed on ice. Cells were isolated by enzymatic dispersion as described previously (Hughes & Takahira, 1998). Briefly, 5 mm-square pieces of RPE–choroid were dissected from the inferior and superior pigmented regions of bovine eyecups and incubated for 30 min at 37 °C in cell isolation medium (135 mM NMDG-Cl, 5 mM KCl, 10 mM Hepes, 3 mM EDTA-KOH, 10 mM glucose, 3 mM cysteine, 0.2 mg ml^{-1} papain (type III), titrated to pH 7.4 with NMDG-free base). The tissue was then incubated in standard bath solution containing 0.1 % BSA for 3 min and finally in standard bath solution alone for another 10 min before dislodging cells by gentle vortexing. As described previously for frog (Hughes & Steinberg, 1990) and human RPE cells (Hughes *et al.* 1995*b*), isolated bovine RPE cells had a 'dumb-bell' shape, with a smooth basolateral membrane domain and an apical membrane domain often containing long processes. Cells were stored in standard bath solution at 4 °C for up to 24 h before use.

Solutions. The standard bath solution for experiments on isolated RPE cells consisted of (mM): 135 NaCl, 5 KCl, 10 Hepes, 10 glucose, 1.8 $CaCl_2$, 1.0 $MgCl_2$, titrated to pH 7.4 with NaOH. To study the dependence of the native Kir conductance on extracellular K^+, $[K^+]_o$ was varied by equimolar replacement with Na^+. In experiments investigating the permeability of Kir conductance to monovalent cations, the control solution consisted of (mM): 140 X, 10 NMDG-Hepes, 10 mM glucose, 1.8 $CaCl_2$, and 1.0 $MgCl_2$, where X is KCl, NaCl, RbCl, LiCl, or CsCl (pH 7.4). In an effort to isolate Kir currents, Cl^- channels and the electrogenic Na^+–HCO_3^- cotransporter were blocked by adding 250 μM 4,4′-diisothiocyanato-stilbene-2,2′-disulfonic acid (DIDS) to all solutions as a concentrated DMSO stock solution (final concentration of DMSO was 0.05 %). In addition, 100 μM $GdCl_3$ was added to block non-specific cation channels. Neither of these blockers had obvious effects on either the kinetics or voltage dependence of inwardly rectifying K^+ currents.

The pipette solution used for whole-cell recording consisted of (mM): 30 KCl, 83 potassium gluconate, 10 Hepes, 5.5 EGTA-KOH, 0.5 $CaCl_2$, 2 $MgCl_2$, 4 ATP dipotassium salt, titrated to pH 7.2 with KOH. The osmolarities of external and internal solutions were 290 ± 10 and 245 ± 5 mosmol (kg H_2O)$^{-1}$, respectively. All chemicals were of reagent grade and obtained from Sigma Chemical except for papain, which was obtained from Aldrich Chemical (Milwaukee, WI, USA).

Electrophysiological recording. Isolated RPE cells were transferred to a continuously perfused Lucite recording chamber on the stage of an inverted microscope (Segawa & Hughes, 1994). All experiments were conducted at room temperature (23–25 °C). Pipettes were pulled from 7052 glass tubing (o.d.= 1.65 mm, i.d. = 1.2 mm, Garner Glass) with a multistage programmable puller and heat-polished to a resistance in the range 1–3 MΩ before use. Membrane currents were recorded using the conventional whole-cell or cell-attached patch recording configuration of the patch-clamp technique (Hamill *et al.* 1981). Currents were amplified with an Axopatch 200 amplifier (Axon Instruments) with the built-in low pass filter set to 1 kHz (unless noted otherwise), digitized and stored on a computer hard drive for later analysis. In whole-cell recordings, series resistance (R_s) and membrane capacitance (C_m) averaged 6.5 ± 5.2 MΩ and 63.4 ± 12.6 pF, respectively ($n = 25$). To minimize voltage errors when recording large inward Rb^+ currents, R_s was compensated 70–80 % with the internal circuitry of the amplifier. Command potentials were generated by software control (pCLAMP 6, Axon Instruments).

In addition to the inwardly rectifying K^+ (Kir) current, most bovine RPE cells also expressed a delayed rectifier K^+ current and some had an M-type K^+ current as well (Takahira & Hughes, 1997). The delayed rectifier current was inactivated by holding the membrane potential at 0 mV between voltage steps and ramps. Cells exhibiting M-type K^+ currents were excluded from the present study.

Voltage-clamp protocols and analysis

Current voltage (I–V) relationships were constructed using data obtained from either voltage-ramp or voltage-step protocols. In the voltage-ramp protocol, the membrane potential was held at 0 mV and then ramped every 15 s from +60 to −160 mV over a 4 s period. In the voltage-step protocol, the membrane potential was held at 0 mV and stepped for 1 s to voltages ranging from +50 to −150 mV in 10 mV steps (oocyte) or from +40 to −160 mV in 20 mV steps (RPE).

Selectivity for monovalent cations was determined under bi-ionic conditions by substituting Rb^+, Na^+, Li^+, or Cs^+ for K^+ in the bathing solution. Permeability ratios, P_X/P_K, were calculated according to a modified form of the Goldman-Hodgkin-Katz voltage equation (Hille, 1992):

$$E_X - E_K = (RT/zF)\ln(P_X/P_K), \quad (1)$$

where E_X is the reversal potential with 98 mM (oocytes) or 140 mM (RPE cells) cation X in the bath, z is the valancy, and R, T and F have their usual meanings. Relative conductance was calculated by measuring the inward slope conductance (g_X) between −140 and −160 mV for each monovalent cation and normalizing it to the slope conductance obtained with K^+ in the bath.

To investigate the relationship between membrane voltage (V_m), conductance and $[K^+]_o$, the chord conductance (G_X) was determined according to the equation:

$$G_X = I/(V_m - E_X), \quad (2)$$

where I is the amplitude of the whole-cell current and E_X is the apparent reversal potential with 98 mM (oocytes) or 140 mM (RPE cells) cation X in the bath.

Non-stationary noise analysis was carried out essentially as described (Heinemann & Conti, 1992; Jackson & Strange, 1996; Traynelis & Jaramillo, 1998). The activity of a specific population of channels gives rise to a macroscopic current (I), which can be defined as:

$$I = N i P_o, \quad (3)$$

where N is the number of channels in the membrane, i is the current flowing through a single channel and P_o is the channel open

probability. Analysis of 'noise' in macroscopic current can be used to estimate the single-channel current (and, therefore, the unitary conductance) and the number of channels in the membrane. Assuming that the membrane contains N independent and identical channels having two conductance states, open and closed, and that graded changes in macroscopic current are due to graded changes in channel open probability, then the current noise or variance, σ^2, is given by:

$$\sigma^2 = iI - I^2/N. \quad (4)$$

By measuring the variance of the mean macroscopic current during different levels of channel activity, channel size and density can be estimated. Because both Kir7.1 and RPE Kir currents are essentially time independent, we applied Ba^{2+}, a voltage-dependent blocker, to produce a time-dependent change in channel open probability.

Data are given as means ± S.E.M. and were fitted using computer software (SigmaPlot 4.0, SPSS Inc., Chicago, IL, USA).

RESULTS

Identification and cloning of human Kir7.1

Random sequencing of cDNA clones from a subtracted bovine RPE cDNA library (Chang *et al.* 1997, 1999) led to the identification of a novel cDNA having sequence similarity with ROMK2. We used this cDNA as a probe to screen a human RPE cDNA library and identified more than 10 positive clones. One of the cDNA clones, pc84, contained the largest cDNA insert (2.4 kb) and was completely sequenced. Analysis of the sequencing data indicated that pc84 contained the entire coding sequence for a Kir7.1 channel subunit as well as a partial 3′ end-sequence (data not shown). The open reading frame encodes a 360-amino acid polypeptide that is identical to that reported previously for human Kir7.1 (Döring *et al.* 1998; Krapivinsky *et al.* 1998; Partiseti *et al.* 1998).

Tissue distribution

Figure 1*A* shows a Northern blot of RNA isolated from various bovine tissues hybridized with a *Kir7.1* probe. A strong 1.6 kb signal was detected in the RPE but not the neural retina or any other tissues examined, despite the fact that the RPE lane contained less RNA (Fig. 1*B*). These results indicate that *Kir7.1* is highly expressed in the RPE. It should be noted, however, that previous studies reported a wider expression pattern for *Kir7.1* (Döring *et al.* 1998; Krapivinsky *et al.* 1998; Partiseti *et al.* 1998; Nakamura *et al.* 1999, 2000). The reason for the apparent difference from our results is unclear. Although our Northern blot did not include several of the tissues in which *Kir7.1* expression has been reported, it did include brain, kidney and testis. It is possible that our Northern blots were less sensitive than the reverse transcription and Northern assays used by others. In addition, the results presented here may reflect species-specific differences in expression pattern because the previous studies were done with rat and/or human tissues while our studies were done with bovine tissues.

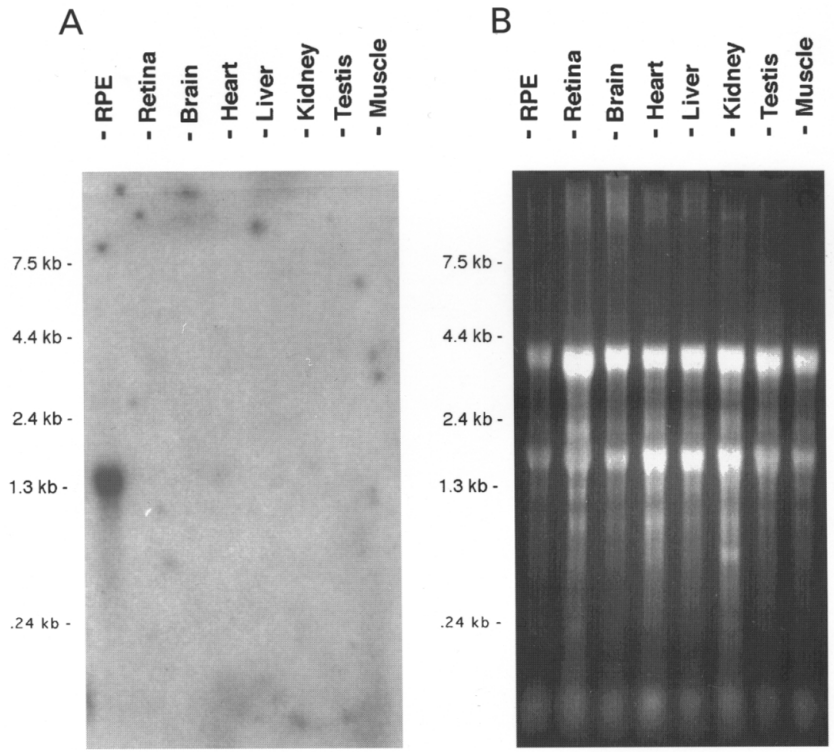

Figure 1. Kir7.1 is highly expressed in the RPE

A, Northern blot analysis of total RNA (10 μg lane^{-1}) extracted from bovine RPE, retina and other tissues and hybridized with human *Kir7.1* probe. *B*, the same RNA gel stained with ethidium bromide.

Functional expression of Kir7.1 in *Xenopus* oocytes

Basic properties

When bathed in the standard 2 mM K^+ solution, Kir7.1 cRNA-injected oocytes typically had a large negative membrane potential and exhibited inwardly rectifying currents. Figure 2*A* (upper panel) depicts a representative family of currents recorded from a Kir7.1 cRNA-injected oocyte. Inward currents activated rapidly in response to hyperpolarizing voltage pulses, whereas outward currents evoked by depolarizing pulses underwent a time-dependent inactivation. The steady-state *I–V* relationship generated by a 4 s voltage ramp in the same oocyte exhibited mild inward rectification, with relatively large outward currents at voltages positive to V_0, the zero current potential (Fig. 2*B*). Addition of 10 mM Ba^{2+} to the bath blocked virtually all of the Kir7.1 current, unmasking an endogenous Ca^{2+}-activated Cl^- current at voltages positive to about −20 mV. For 10 Kir7.1 cRNA-injected oocytes, V_0 averaged −99.5 ± 6.8 mV and the chord conductance (G) measured at −160 mV averaged 18.4 ± 1.5 μS (mean ± S.E.M.).

Permeation properties

Previous studies by Krapavinsky *et al.* (1998) and Döring *et al.* (1998) showed that, unlike other native and cloned Kir channels, the macroscopic Kir7.1 conductance exhibits a low dependence on extracellular K^+ concentration ($[K^+]_o$). In addition, Wischmeyer *et al.* (2000) recently reported that although Kir7.1 has a monovalent cation permeability sequence of $K^+ > Rb^+$, it has a macroscopic Rb^+ conductance that is about 8-fold larger than its K^+ conductance. To allow a direct comparison to the native Kir conductance in RPE cells (see *Properties of native Kir channels in bovine RPE* below), we re-examined the dependence of macroscopic Kir7.1 conductance on $[K^+]_o$ as well as its permselectivity to monovalent cations.

Figure 3*A* shows a series of representative *I–V* relationships obtained from a single Kir7.1 cRNA-injected oocyte. Increases in $[K^+]_o$ caused positive shifts in V_0 and decreased the slope of the *I–V* relationship in the vicinity of V_0. Outward currents, however, were affected, becoming smaller as $[K^+]_o$ was increased. Figure 3*B* plots the mean values of V_0 ($n = 6$) as a function of $[K^+]_o$, and the straight line is the least squares fit of the data with a slope of 55.6 mV per 10-fold change in $[K^+]_o$. This K^+-induced change in V_0 coincides well with the change in E_K calculated by the Nernst equation (58 mV), indicating that the Kir7.1 conductance is highly selective for K^+ over Na^+.

To evaluate the dependence of Kir7.1 conductance on $[K^+]_o$, we calculated chord conductance (G) from the data in Fig. 3*A* and plotted it as a function of membrane voltage (V). Figure 3*C* shows that both the shape of the *G–V* curve and its position along the *x*-axis changed as $[K^+]_o$ was varied. In the presence of 1 and 2 mM K^+, the shape of the *G–V* curve was sigmoidal, but at higher

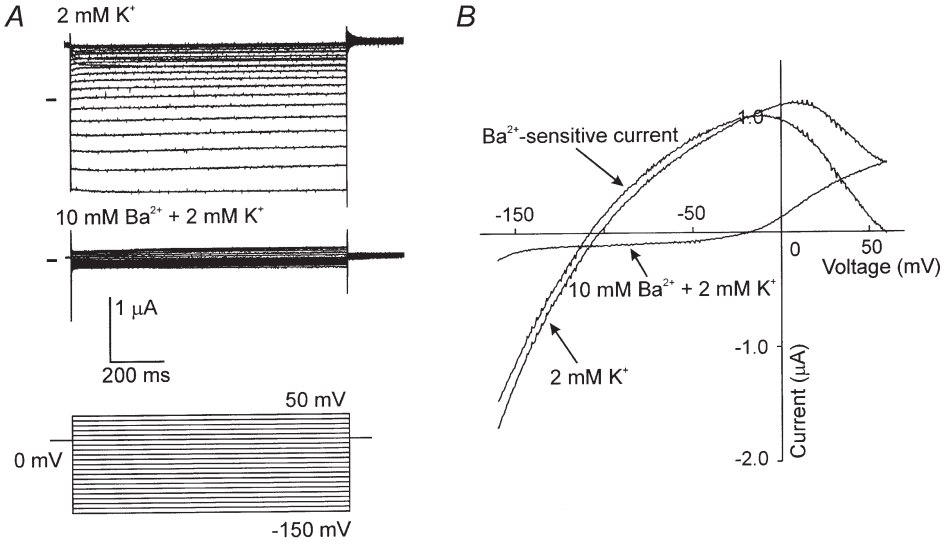

Figure 2. Characterization of macroscopic Kir7.1 currents

A, families of currents measured from a Kir7.1 cRNA-injected *Xenopus* oocyte bathed with standard (2 mM K^+) solution in the absence (upper panel) and presence (middle panel) of 10 mM Ba^{2+}. The horizontal line to the left of the records indicates the zero-current level. The voltage protocol used to evoke these currents is shown below. *B*, *I–V* relationships obtained from the same oocyte using the voltage-ramp method.

concentrations the curve was exponential, perhaps because the test voltages were not large enough to produce saturation. As a consequence of the G–V curves crossing over at large negative potentials, the relationship between $[K^+]_o$ and conductance depended on voltage. At −160 mV, the most negative voltage examined, chord conductance increased slightly with increasing $[K^+]_o$, as reported previously (Döring *et al.* 1998). In contrast, at more positive potentials, the macroscopic Kir7.1 conductance decreased with increasing $[K^+]_o$.

In order to differentiate between the effects of $[K^+]_o$ on outward and inward conductances, we re-plotted the data as a function of driving force, $V_m - E_K$ (Fig. 3*D*). The results demonstrate that at voltages near E_K, both outward and inward conductances decreased with increasing $[K^+]_o$, although the changes were small at concentrations greater than 50 mM. Similar results were obtained in five other oocytes. This behaviour is contrary to that of other members of the Kir channel family, whose macroscopic conductance typically saturates with voltage and increases in proportion to the square root of $[K^+]_o$. The mechanism underlying the unusual behaviour of Kir7.1 is not known, but obviously must involve changes in single-channel conductance, open probability, or both.

We investigated the permselectivity of Kir7.1 channels under bi-ionic conditions by superfusing oocytes with solutions containing various monovalent cations (intracellular $[K^+]$ was presumed to remain constant). Figure 4*A* shows families of whole-cell currents recorded from an oocyte bathed with either K^+, Rb^+, Li^+, Na^+, or Cs^+ as the sole monovalent cation; the corresponding I–V relationships averaged from nine oocytes are shown in Fig. 4*B* and, at a different scale, Fig. 4*C*. Compared to the currents in K^+, the maximal inward currents in Na^+, Li^+ and Cs^+ external solutions were smaller, whereas those in Rb^+ were nearly 10 times larger. It is interesting to note that at depolarized voltages, the Rb^+ slope conductance was actually somewhat smaller than the K^+ conductance (not apparent in averaged experiments) and that it increased dramatically near −50 mV, roughly 40 mV negative to the apparent reversal potential. The significance of this

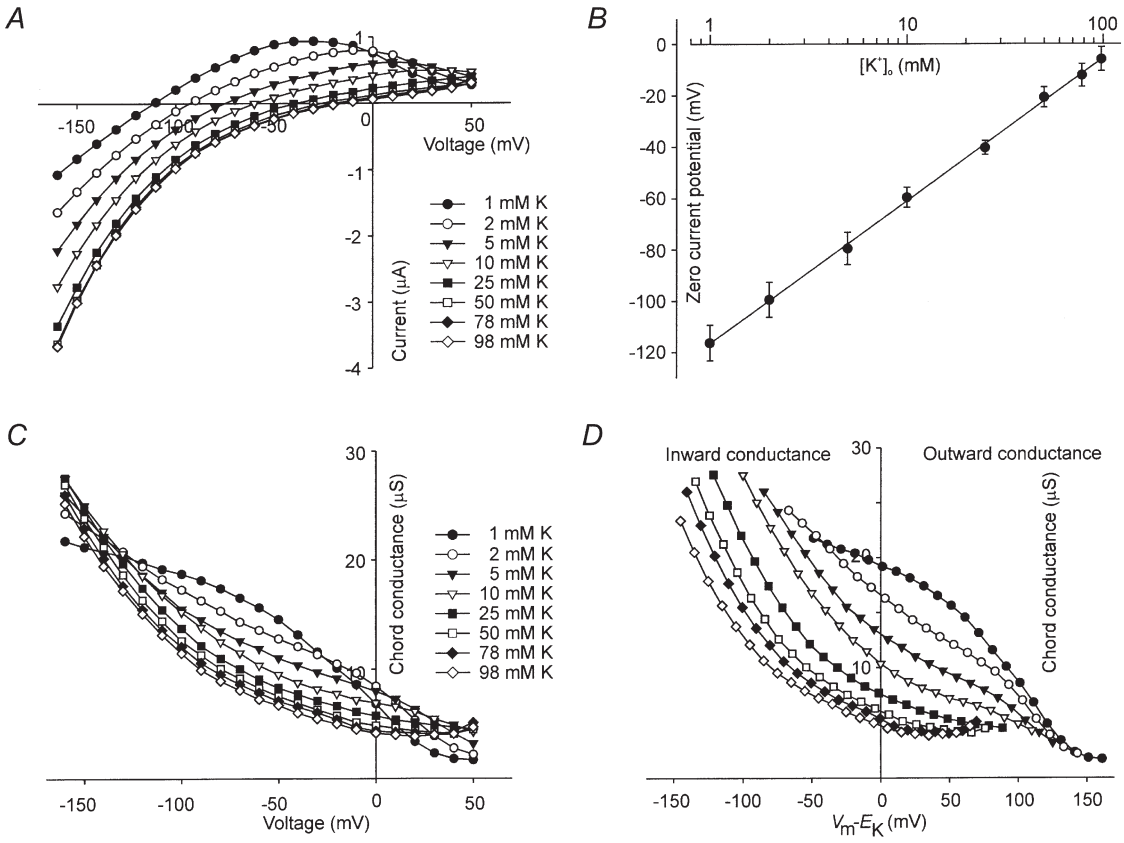

Figure 3. Dependence of Kir7.1 current and conductance on $[K^+]_o$

A, current–voltage relationships obtained from a single Kir7.1 cRNA-injected oocyte bathed with various $[K^+]_o$. Data were generated from currents evoked by voltage steps. *B*, relationship between zero current potential and $[K^+]_o$. Each filled circle and vertical bar indicates the mean and S.E.M. for 12 oocytes. The continuous line shows the linear regression fit to the data. *C*, relationship between conductance and membrane voltage. Chord conductance was calculated from the data in *A*. *D*, relationship between conductance and driving force. The same data in *C* plotted as a function of $V_m - E_K$.

'activation potential' is unclear, but may reflect channel gating or the relief from block by some intracellular ion. The selectivity sequence calculated from relative slope conductances (g_X/g_K) in the voltage range −140 to −160 mV was: Rb^+ (9.5) ≫ K^+ (1.0) > Na^+ (0.46) > Cs^+ (0.33) > Li^+ (0.14) (Table 1). These results are similar to those previously reported by Wischmeyer *et al.* 2000).

Replacement of external K^+ with Na^+, Li^+, or Cs^+ caused V_0 to shift to more negative potentials, whereas replacement with Rb^+ left V_0 virtually unchanged (Fig. 4*C*). Although it is common to substitute V_0 for reversal potential (E_{rev}) in the calculation of permeability ratios (eqn (1)), this practice can lead to significant errors due to the impact of endogenous channels, particularly when the current of interest is small. In an attempt to circumvent this problem, we applied 10 mM Ba^{2+} to the bath in the presence of various monovalent cations and measured the reversal potential of Ba^{2+}-sensitive currents. When Na^+, Li^+, or Cs^+ was in the bath, E_{rev} was significantly more negative than the corresponding value of V_0 (Fig. 5*C*, *D* and *E*; Table 1). In contrast, when K^+ or Rb^+ was in the bath, E_{rev} could not be estimated by this method because the Ba^{2+}-induced block of current was strongly voltage dependent (Fig. 5*A* and *B*). The relationship between V_0 and $\log[K^+]_o$ (Fig. 3*B*) indicates

Table 1. Permeability and conductance ratios for the Kir7.1 conductance

Ion (X)	V_0 (mV) ($n = 9$)	E_{rev} (mV) ($n = 5$)	P_X/P_K	g_X/g_K
K^+	−8.4 ± 2.3	—	1	1
Rb^+	−10.8 ± 1.1	—	0.886 ± 0.045	9.503 ± 1.548
Na^+	−136.9 ± 6.4	−156.1 ± 3.3	0.003 ± 0.001	0.458 ± 0.011
Li^+	−126.6 ± 5.6	−160.5 ± 2.0	0.002 ± 0.001	0.139 ± 0.012
Cs^+	−37.6 ± 3.7	−116.6 ± 3.2	0.013 ± 0.004	0.331 ± 0.035

that for external K^+, E_{rev} must lie close to the measured value of V_0. Assuming that this is also true for Rb^+, we obtain a permeability sequence of K^+ (1.0) ≈ Rb^+ (0.89) > Cs^+ (0.013) > Na^+ (0.003) ≈ Li^+ (0.002) ($n = 5$) (Table 1), in agreement with the results of Wischmeyer *et al.* (2000).

In addition to changes in V_0 and inward slope conductance, substitution of K^+ with other monovalent cations also affected the size of outward currents (Fig. 4*C*). The magnitude of outward current was considerably larger in the presence of extracellular Na^+ or Li^+ than it was in K^+, Rb^+, or Cs^+, and most of this current was blocked by 10 mM Ba^{2+} (Fig. 5*C* and *D*), indicating that it represented outward K^+ current through Kir7.1 channels. The magnitude of outward Kir7.1 current in the presence of

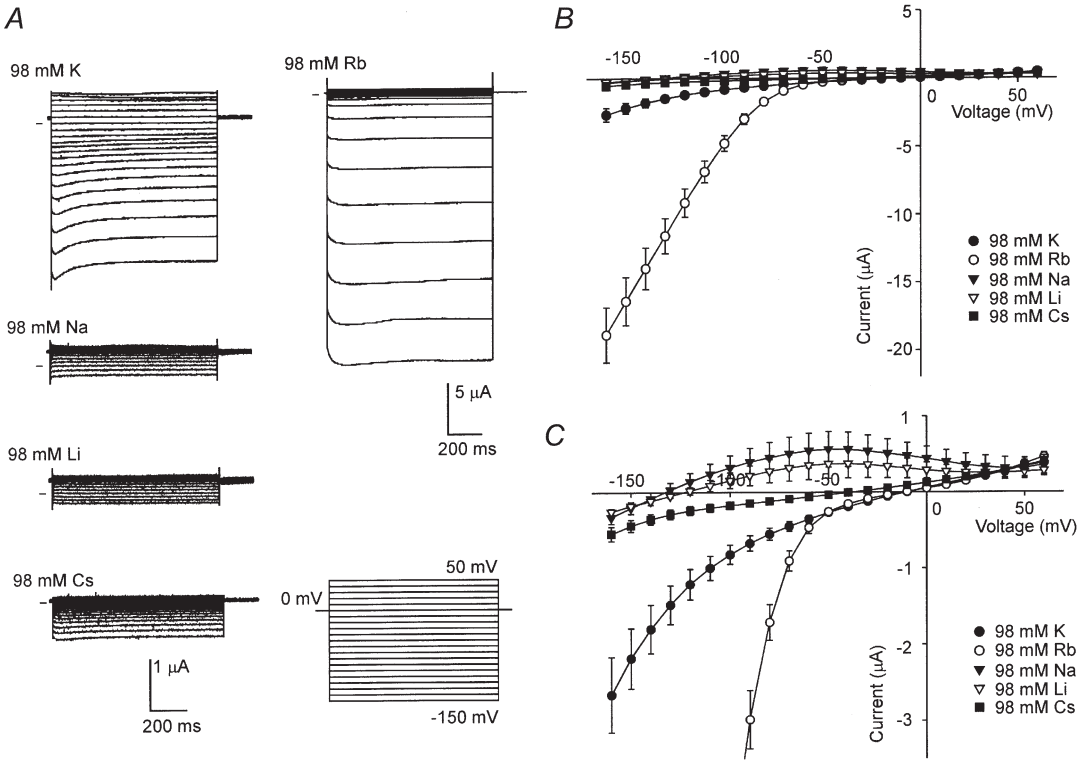

Figure 4. Effect of cation substitution on Kir7.1 conductance

A, macroscopic currents recorded from a representative Kir7.1 cRNA-injected oocyte bathed in 98 mM K^+, Na^+, Li^+, Cs^+, or Rb^+. Currents were evoked by the voltage-step protocol indicated. *B*, current–voltage relationships obtained with various monovalent cations in the bath. Each point and vertical bar represents the mean ± S.E.M. for 9 oocytes. *C*, same data as in *B* but at a higher gain to show zero current potentials. Connecting lines have no theoretical significance.

external K^+ or Rb^+ is difficult to estimate because the Ba^{2+}-induced block was strongly voltage dependent in these cases. It seems likely, however, that a significant fraction of K^+ outward current observed in the presence of external K^+ or Rb^+ was mediated by endogenous channels. In the presence of external Cs^+, only inward currents at large negative potentials were blocked (Fig. 5*E*), suggesting that Cs^+ behaves as a permeant blocker. We conclude that outward K^+ current through Kir.71 channels is considerably greater in the presence of external Na^+ and Li^+ than it is in the presence of external K^+, Rb^+, or Cs^+. The reason for these differences is unclear, but the mechanism might involve specific cation interactions with extracellular domains of the channel, influencing gating or perhaps the permeation pathway itself.

Non-stationary noise analysis

In a previous study on Kir7.1 channels expressed in mammalian cells, Krapivinsky and colleagues (1998) recorded currents from cell-attached patches and used non-stationary noise analysis to estimate that Kir7.1 has a single-channel conductance of ~50 fS. We attempted to confirm these results in cell-attached recordings from Kir7.1 cRNA-injected oocytes, but when the pipette contained 98 mM K^+, we failed to observe inwardly rectifying currents in 12 patches. Because the macroscopic Kir7.1 current increased roughly 10-fold when Rb^+ was substituted for K^+ (Fig. 4), we reasoned that Kir7.1 currents in cell-attached patches might be better resolved by using Rb^+ as the charge carrier. Indeed, when K^+ in the pipette was replaced with Rb^+, we routinely recorded inwardly rectifying currents. Figure 6*A* shows

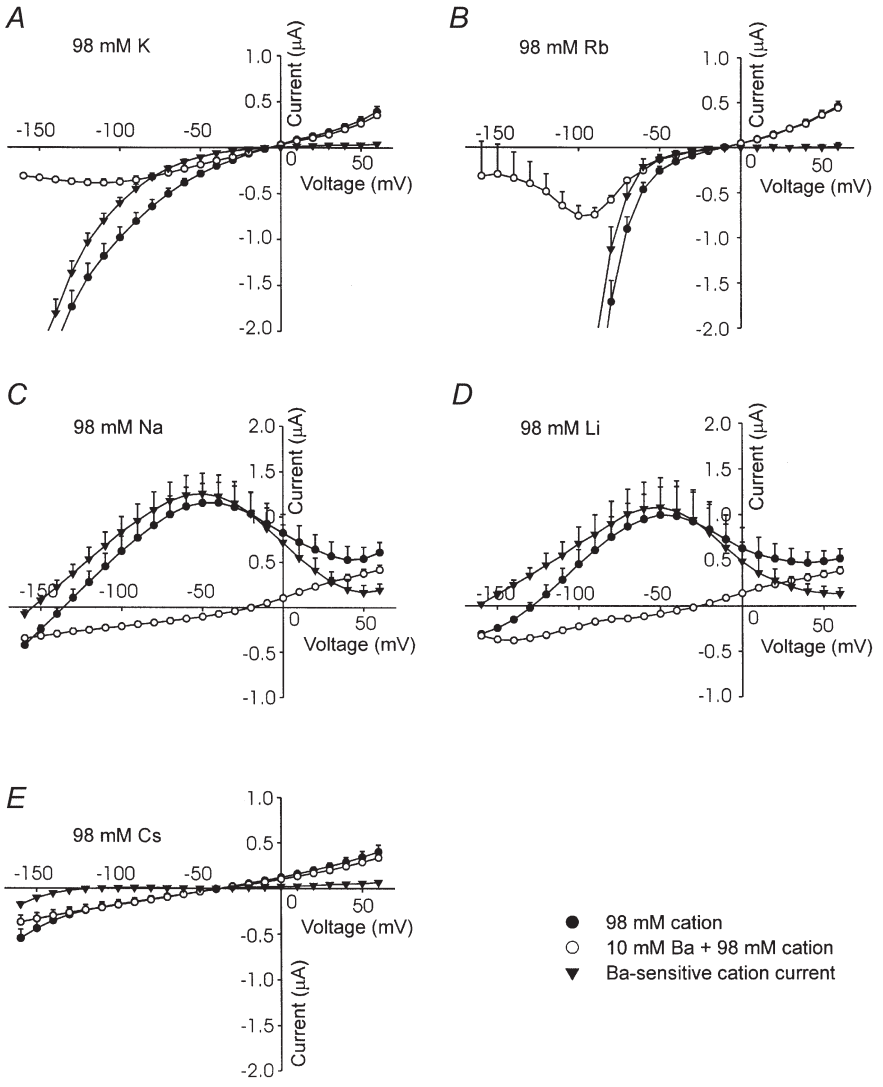

Figure 5. Determination of the reversal potential of Kir7.1 currents from Ba^{2+}-sensitive currents

Panels depict averaged *I–V* relationships obtained in the presence and absence of 10 mM Ba^{2+} with either 98 mM K^+ (*A*), Rb^+ (*B*), Na^+ (*C*), Li^+ (*D*) or Cs^+ (*E*) as the sole monovalent cation ($n = 5$). Ba^{2+}-sensitive currents are also depicted.

representative recordings obtained with 98 mM Rb^+ and 1 mM Ba^{2+} in the recording pipette. Instantaneous currents were inwardly rectifying, with a sharp increase in conductance at about −50 mV (Fig. 6*B*, ○), reminiscent of whole-cell Rb^+ currents (Fig. 4*B*). Inward Rb^+ currents exhibited a time-dependent decay due to a voltage-dependent block by Ba^{2+} (Fig. 6*C*, ●), allowing the estimation of single-channel current (i) and number of channels (N) by non-stationary noise analysis. Figure 6*C* plots current variance *vs.* mean current amplitude calculated from 40 successive current records elicited by voltage steps from 0 mV to −100 mV and the smooth curve is the least squares fit of the data to eqn (4), with values for i and N of 0.31 pA and 2861, respectively. Similar results were obtained in five other cell-attached patches, yielding an average single-channel chord conductance of 2.27 ± 0.26 pS.

Properties of native Kir channels in bovine RPE

Basic properties

As reported previously, isolated bovine RPE cells exhibited a prominent inwardly rectifying K^+ current (Hughes & Takahira, 1998). Figure 7 shows that in the presence of 5 mM $[K^+]_o$, the I–V relationship was mildly inwardly rectifying, with substantial outward currents at voltages positive to V_0. Most of this current was blocked by the addition of 10 mM Ba^{2+} to the bath, which unmasked a small outwardly rectifying current that reversed near the Cl^- equilibrium potential.

Permeation properties

We previously showed that the Kir conductances in toad (Segawa & Hughes, 1994) and human RPE cells (Hughes & Takahira, 1996) are inversely dependent on extracellular $[K^+]_o$. We confirmed and extended these findings in bovine RPE cells by measuring changes in conductance over a wider range of $[K^+]_o$. Figure 8*A* shows that increasing $[K^+]_o$ shifted the I–V relationship obtained from a representative cell to the right and decreased the slope of the I–V relationship near V_0. A plot of V_0 *vs.* $\log[K^+]_o$ (Fig. 8*B*) revealed a linear relationship that was close to that predicted by the Nernst equation (55.6 mV *vs.* 58 mV per 10-fold change in $[K^+]_o$), indicating that under our present recording conditions, the K^+

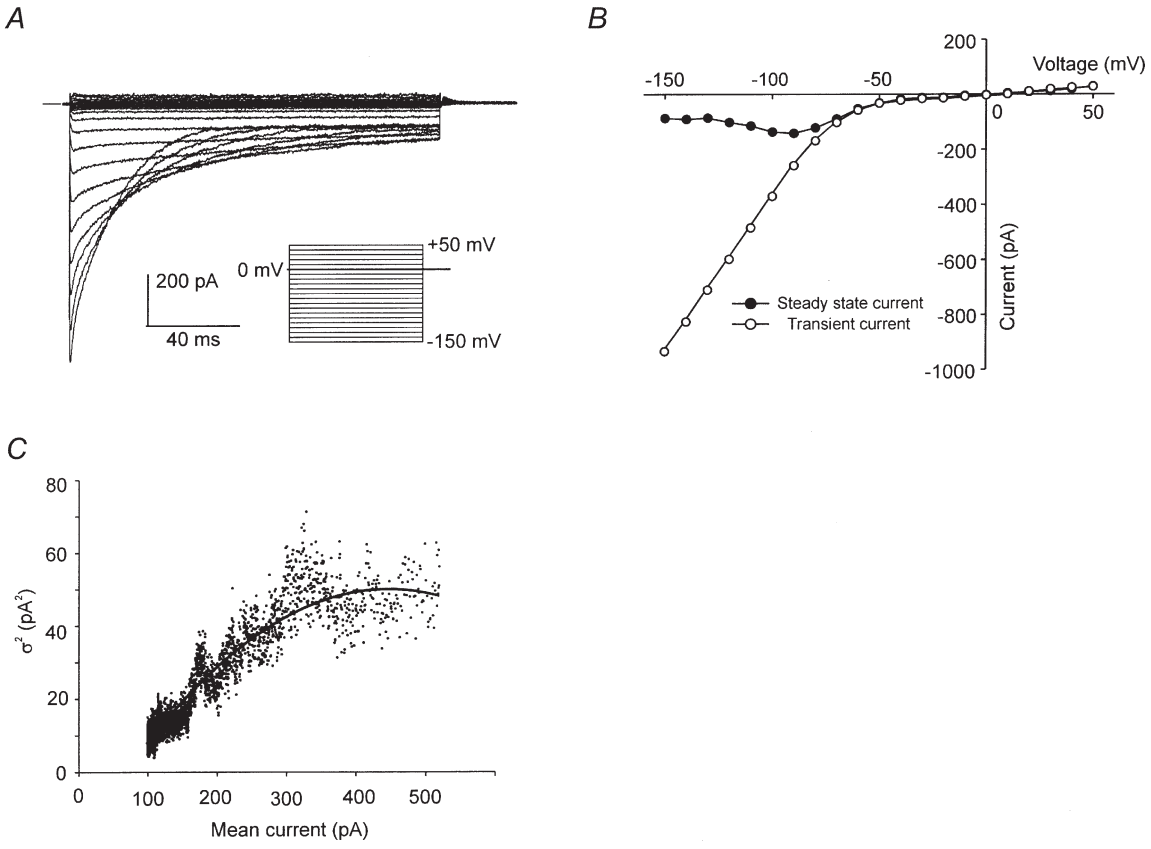

Figure 6. Non-stationary noise analysis of Kir7.1 Rb^+ currents

A, family of currents recorded from a cell-attached patch on a Kir7.1 cRNA injected oocyte with 98 mM Rb^+ and 1 mM Ba^{2+} in the pipette. The bath contained 98 mM K^+ external solution to depolarize the membrane potential. *B*, I–V relationships obtained from the currents in *A* measured 2.5 ms (○) and 167 ms (●) after the onset of the voltage step. *C*, relationship between current variance (σ^2) and mean current from the same patch as in *A*. See text for additional details.

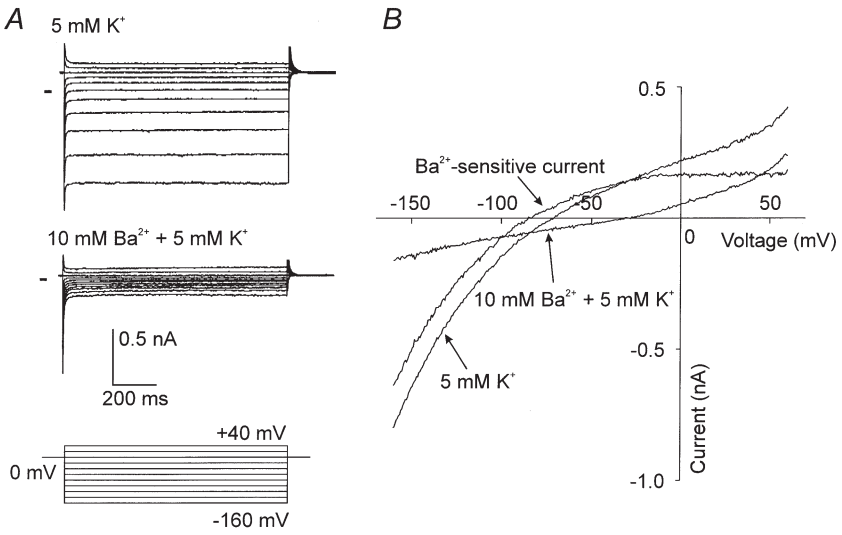

Figure 7. Properties of the Kir current in the RPE

A, families of whole-cell currents recorded from an isolated bovine RPE bathed with standard (5 mM K^+) solution in the absence (upper panel) and presence of 10 mM Ba^{2+} (middle panel). The voltage protocol used to evoke these currents is shown below. *B*, *I–V* relationships obtained from the same cell as in *A* using a voltage-ramp protocol.

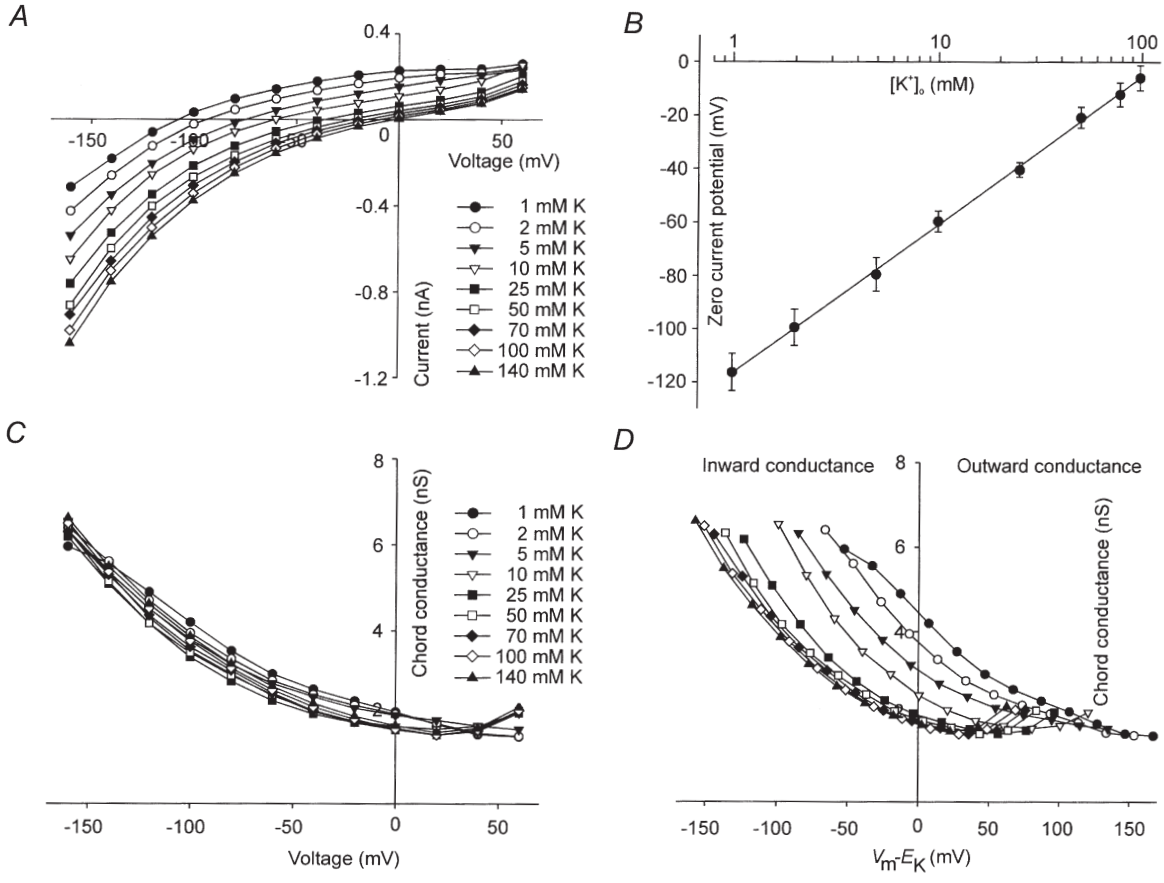

Figure 8. Dependence of RPE Kir currents on $[K^+]_o$

A, *I–V* relationships obtained from a single bovine RPE cell bathed with various $[K^+]_o$. Data were generated from currents evoked by voltage steps. *B*, relationship between zero current potential and $[K^+]_o$. Each filled circle and vertical bar indicates the mean ± S.E.M. for 8 cells. The continuous line shows the linear regression fit to the data. *C*, relationship between conductance and membrane voltage. Chord conductance was calculated from the data in *A*. *D*, relationship between conductance and driving force. The same data in *C* plotted as a function of $V_m - E_K$.

conductance accounted for roughly 95% of the whole-cell conductance of bovine RPE cells.

To evaluate the dependence of the Kir conductance on $[K^+]_o$ and voltage, we calculated chord conductance from the data in Fig. 8*A* and plotted it as a function of membrane voltage (Fig. 8*C*). The *G–V* curve was nearly the same at all K^+ concentrations, although conductance at given voltage in the range −120 to + 10 mV was slightly higher at lower concentrations. When conductance was plotted as a function of driving force (Fig. 8*D*), an effect $[K^+]_o$ on inward and outward conductances could be clearly seen. In the K^+ concentration range 1–25 mM, inward and outward conductances decreased with increases in $[K^+]_o$, but they changed little when $[K^+]_o$ was increased further. Similar results were obtained in five other cells. Thus, despite some quantitative differences, the RPE Kir conductance responds to changes in $[K^+]_o$ in a manner that is qualitatively similar to that of Kir7.1 but opposite to that typical of other Kir channels.

In addition to its similarity to the Kir7.1 conductance with regard to its inverse dependence on $[K^+]_o$, the RPE

Table 2. Permeability and conductance ratios for the RPE Kir conductance

Ion (X)	V_0 (mV) ($n = 11$)	E_{rev} (mV) ($n = 5$)	P_X/P_K	g_X/g_K
K^+	−7.3 ± 0.7	—	1	1
Rb^+	−10.4 ± 1.3	—	0.811 ± 0.138	8.889 ± 0.041
Na^+	−141.9 ± 2.4	−153.2 ± 6.3	0.003 ± 0.001	0.585 ± 0.097
Li^+	−123.1 ± 1.8	−157.4 ± 3.3	0.002 ± 0.001	0.083 ± 0.012
Cs^+	−41.4 ± 2.9	−105.8 ± 3.9	0.021 ± 0.006	0.225 ± 0.053

Kir conductance also shares other unusual permeation properties. Figure 9*A* shows a representative family of *I–V* relationships recorded from a single bovine RPE cell under bi-ionic conditions. For all monovalent cations tested, the *I–V* curve showed inward rectification, but the magnitude of inward currents was substantially greater when Rb^+ was in the bath (Fig. 9*B*). As was true for the macroscopic Kir7.1 conductance, inward Rb^+ current through RPE Kir conductance exhibited an activation potential near −50 mV. The selectivity sequence calculated from inward slope conductances in the voltage range −140 to −160 mV was: Rb^+ (8.9) ≫ K^+ (1.0) > Na^+

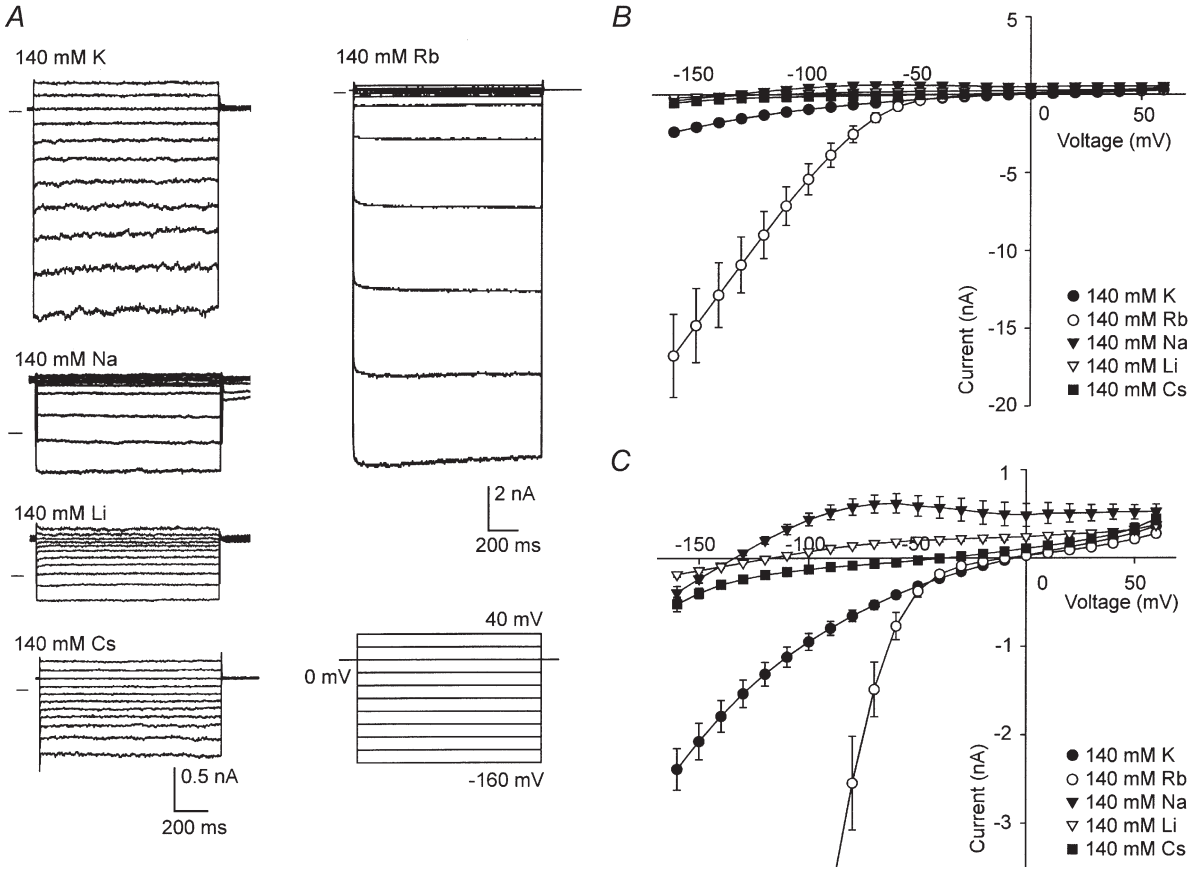

Figure 9. Effect of cation substitution on the RPE Kir conductance

A, macroscopic currents recorded from a representative bovine RPE cell bathed in 140 mM K^+, Na^+, Li^+, Cs^+, or Rb^+. Currents were evoked by the voltage-step protocol indicated. *B*, *I–V* relationships obtained with various monovalent cations in the bath. Each point and vertical bar represent mean and S.E.M. for 11 RPE cells. *C*, same data as in *B* but at a higher gain to show zero current potentials. Connecting lines have no theoretical significance.

(0.59) > Cs^+ (0.23) > Li^+ (0.08) (Table 2). These values are nearly identical to those obtained for Kir7.1 (Table 1).

Figure 9*C* depicts the same *I–V* curves as in Fig. 9*B* but at a higher gain to show the effect of cation substitution on V_0. Replacement of external K^+ with Rb^+ had little effect on V_0, but replacement with Na^+, Li^+, or Cs^+ caused V_0 to shift to more negative potentials (Table 2). Because of the influence of residual Cl^- and Na^+ currents, these changes in V_0 may underestimate the actual changes in E_{rev}. Therefore, we applied 10 mM Ba^{2+} in the continued presence of the various monovalent cations (Fig. 10) to allow the estimation of E_{rev} from the reversal of Ba^{2+}-sensitive currents. When K^+ or Rb^+ was in the bath, the Ba^{2+} block was strongly voltage dependent, making it impossible to estimate E_{rev} from Ba^{2+}-sensitive currents. With external Cs^+, Na^+, or Li^+, however, the Ba^{2+}-sensitive current reversed at a potential that was significantly more negative than the corresponding value of V_0 (Fig. 10*C*, *D* and *E*; Table 2). Using these E_{rev} values for external Cs^+, Na^+ and Li^+ and V_0 values for K^+ and Rb^+, we calculate a permeability sequence of K^+ (1.0) ≈ Rb^+ (0.81) > Cs^+ (0.021) > Na^+ (0.003) ≈ Li^+ (0.002) (Table 2), which is nearly identical to that obtained for the cloned Kir 7.1 channel (Table 1).

The magnitude of outward currents also varied depending on the species of cation in the bath, being considerably larger in the presence of external Na^+ and, to a lesser extent, Li^+, than in the presence of K^+, Rb^+, or Cs^+ (Fig. 9*C*). External Ba^{2+} blocked the outward currents present with Na^+ or Li^+ in the bath (Fig. 10*C* and *D*), but

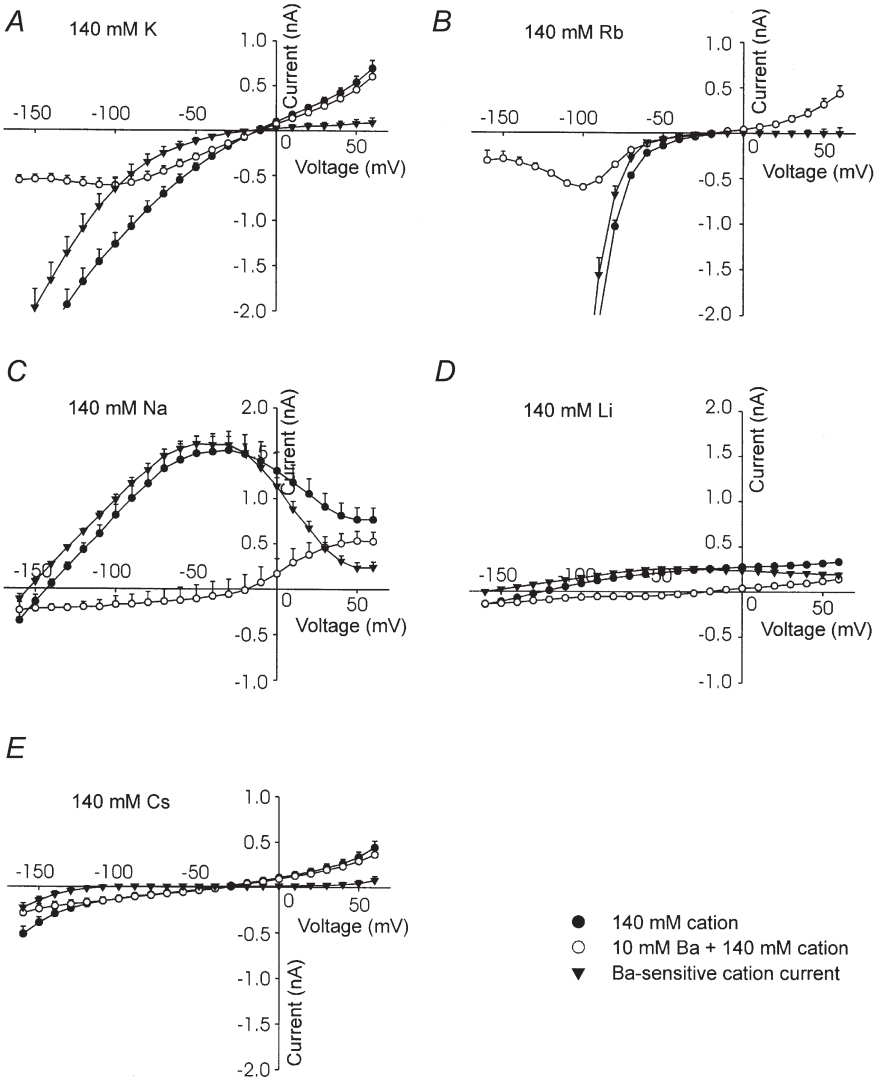

Figure 10. Determination of the reversal potential of RPE Kir currents from Ba^{2+}-sensitive currents

Panels depict averaged *I–V* relationships obtained in the presence and absence of 10 mM Ba^{2+} with either 140 mM K^+ (*A*), Rb^+ (*B*), Na^+ (*C*), Li^+ (*D*) or Cs^+ (*E*) as the sole monovalent cation ($n = 11$). Ba^{2+}-sensitive currents are also depicted.

had little effect on outward currents in the presence of K^+, Rb^+, or Cs^+ (Fig. 10*A*, *B* and *E*). Thus, like the cloned Kir7.1 channel, the RPE Kir channel appears to conduct outward K^+ current when either Na^+ or Li^+ is the sole monovalent cation in the bath, but little or no outward current when the bath contains K^+, Rb^+, or Cs^+.

Non-stationary noise analysis and localization of Kir channels to the RPE apical membrane

Electrophysiological studies on the intact RPE have demonstrated that the apical membrane has a large K^+ conductance (Lasansky & De Fisch, 1966; Miller, Steinberg & Oakley, 1978; Joseph & Miller, 1991) that is probably composed of inwardly rectifying channels (Hughes *et al.* 1995*a*). In numerous recordings from cell-attached patches of apical membrane on isolated bovine RPE cells, however, we failed to record unitary currents that could be attributed to a Kir channel, suggesting that the channel underlying the macroscopic Kir current may have a very low conductance. Consistent with this idea, the 'leak' current in some patches exhibited inward rectification (data not shown), but this was not studied further because of the low frequency of these observations. When we substituted Rb^+ for K^+ in the pipette, however, we routinely observed inwardly rectifying currents in apical membrane patches. Figure 11*A* shows a representative family of currents recorded from a cell-attached apical membrane patch with 140 mM Rb^+ plus 1 mM Ba^{2+} in the pipette. Instantaneous currents were inwardly rectifying, with a sharp increase in conductance at about −50 mV (Fig. 11*B*). With prolonged hyperpolarization, inward currents decayed with a mono-exponential time course, reflecting the voltage-dependent block of Kir channels by Ba^{2+}. Similar results were observed in nine of 12 apical membrane patches but in only one of 13 basolateral membrane patches. Hence, inwardly rectifying K^+ channels appear to be localized to the apical membrane of the RPE.

Figure 11*C* shows the results of non-stationary noise analysis of Kir currents recorded from the same apical membrane patch as that depicted in Fig. 11*A* and *B*. Mean current and variance were calculated from 40 current records evoked by voltage steps to −150 mV from a

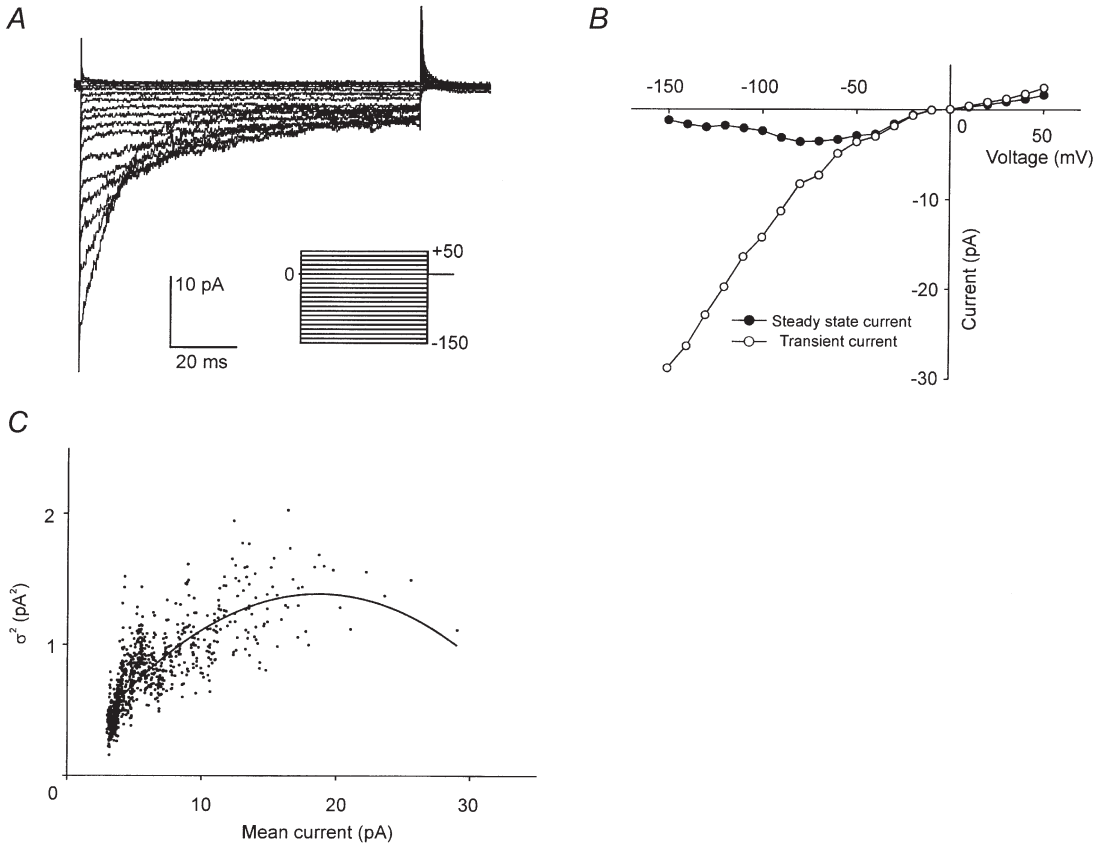

Figure 11. Non-stationary noise analysis of RPE Kir Rb^+ currents

A, family of currents recorded from a cell-attached patch on the apical membrane of a bovine RPE cell with 140 mM Rb^+ and 1 mM Ba^{2+} in the pipette. The bath contained 140 mM K^+ external solution to depolarize the membrane potential. *B*, *I–V* relationships obtained from the currents in *A* measured 2.5 ms (○) and 167 ms (●) after the onset of the voltage step. *C*, relationship between current variance and mean current from the same patch as in *A*. See text for additional details.

holding potential of 0 mV. The smooth curve is the least-squares fit of the data to eqn (4), with values for single-channel current (i) and number of channels (N) of 0.312 pA and 106, respectively. For a total of five apical membrane patches, the unitary chord conductance calculated from estimates of single-channel current averaged 1.70 ± 0.27 pS. Hence, the RPE Kir channel has single-channel Rb^+ conductance that is nearly identical to that of the cloned Kir7.1 channel. From this unitary Rb^+ conductance and the whole-cell Rb^+ chord conductance (104 ± 16.8 nS at −150 mV, $n = 8$), we estimate that each RPE cell contains at least 61 000 Kir channels.

DISCUSSION

We have cloned and sequenced human Kir7.1 from an RPE cDNA library and demonstrated by Northern analysis that Kir7.1 is highly expressed in the RPE. In electrophysiological experiments, we determined that native Kir channels in isolated bovine RPE cells share several unusual permeation properties with heterologously expressed Kir7.1 channels, including an inverse dependence of macroscopic conductance on $[K^+]_o$, a Rb^+-to-K^+ conductance ratio of ∼10 and a low single-channel Rb^+ conductance of ∼2 pS. Finally, in cell-attached patch recordings, we have localized inwardly rectifying Rb^+ currents to the apical membrane of the RPE. Hence, a major conclusion of this paper is that Kir7.1 channel subunits comprise the Kir conductance of the RPE apical membrane.

Cloning of human Kir7.1 from the RPE

In a 'subtracted' bovine RPE cDNA library (Chang *et al.* 1997, 1999), we identified a clone containing a partial sequence with homology to the Kir channel subunit ROMK2. Subsequently, we used this clone to probe a human RPE cDNA library and isolated a cDNA containing the entire open reading frame encoding a 360-amino acid polypeptide identical to Kir7.1, a new member of the Kir gene family (Döring *et al.* 1998; Krapivinsky *et al.* 1998; Partiseti *et al.* 1998; Nakamura *et al.* 1999). Kir7.1 is the most divergent member of the Kir family, with only a 38% sequence identity at the amino acid level with its closest homologue, human Kir1.3 (Shuck *et al.* 1997). While Kir7.1 contains structural motifs typical of inwardly rectifying K^+ channels, namely two membrane spanning domains and an intervening pore domain, its sequence in the pore region diverges at three locations that are conserved in other cloned Kir channel subunits: S111, M125 and G129 (Krapivinsky *et al.* 1998). It is now well established that M125, which lies two residues downstream from the pore selectivity sequence G-Y-G, is responsible for many of the unique permeation properties of the Kir7.1 channel, including a low dependence of macroscopic conductance on $[K^+]_o$ (Döring *et al.* 1998; Krapivinsky *et al.* 1998), a low single-channel conductance (Krapivinsky *et al.* 1998) and a high Rb^+-to-K^+ conductance ratio (Wischmeyer *et al.* 2000).

Tissue distribution of bovine Kir7.1

We evaluated the tissue distribution of *Kir7.1* by Northern blot analysis of mRNA isolated from various bovine tissues. A single transcript of ∼1.4 kb was present in the RPE, but Kir7.1 mRNA could not be detected in neural retina, brain, heart, liver, kidney, testis, or skeletal muscle. These results differ somewhat from reports by other investigators. In a study by Doring *et al.* (1998), three Kir7.1 transcripts were detected in Northern blots of rat mRNA, with a 1.4 kb signal in brain, lung and kidney, a 2.4 kb band in testis and a 3.2 kb band in lung and kidney. In contrast, Northern blot analysis of human RNA detected a single 3.2 kb transcript in brain, small intestine, hippocampus, medulla and thyroid (Partiseti *et al.* 1998; Nakamura *et al.* 1999). These inter- and intra-species differences in the size of Kir7.1 transcripts may reflect different lengths in untranslated regions or poly(A)$^+$ tails (Nakamura *et al.* 2000). Our failure to detect Kir7.1 mRNA in any tissue other than the RPE may be due to the limited exposure time of the blot, or may reflect species-specific differences in expression pattern between rats, cows and humans. This does not affect our conclusion, however, that Kir7.1 is highly expressed in the RPE.

Permeation properties of Kir7.1

Kir7.1 has unique properties with respect to permeant ions. Other native and cloned Kir channels typically exhibit saturation of conductance with voltage and a limiting conductance that is proportional to the square root of $[K^+]_o$ (Lopatin & Nicholas, 1996). In previous studies by other investigators, it was noted that the macroscopic Kir7.1 conductance has an unusually low dependence on $[K^+]_o$ (Döring *et al.* 1998; Krapivinsky *et al.* 1998). Although our results generally agree with this assessment, they reveal that the relationship between Kir7.1 conductance and $[K^+]_o$ is more complex than was previously appreciated. We found that the macroscopic Kir7.1 conductance was non-saturating except at low K^+ concentrations (1 and 2 mM) and exhibited a low dependence on $[K^+]_o$ at very negative potentials (−160 mV) but an inverse dependence on $[K^+]_o$ at voltages positive to about −125 mV. Thus, at physiological voltages, the macroscopic Kir7.1 conductance decreases as $[K^+]_o$ is increased. Obviously, additional information about how single Kir7.1 channel conductance and gating vary with voltage and $[K^+]_o$ are needed before the mechanism(s) responsible for this unconventional behaviour can be elucidated.

In general, the permeation properties of ion channels can be probed in two fundamentally different ways: reversal potentials determined under bi-ionic conditions yield relative permeabilities, whereas current–voltage relationships provide relative conductances. In agreement with the recent report by Wischmeyer *et al.* (2000), we found that Kir7.1 has a Rb^+-to-K^+ permeability ratio of about 1, but a macroscopic Rb^+-to-K^+ conductance ratio of

roughly 10. This is in striking contrast to most other native and cloned Kir channels in which Rb^+ acts as a permeant blocker, giving rise to Rb^+-to-K^+ conductance ratios in the range 0.1–0.5 (Standen & Stanfield, 1980; Zhou *et al.* 1994; Reuveny *et al.* 1996; Löffler & Hunter, 1997; Welling, 1997; Choe *et al.* 1998). It is interesting to note that the macroscopic Rb^+ conductance of Kir7.1 exceeded the K^+ conductance only at voltages negative to about −50 mV; at more positive potentials the Rb^+ and K^+ conductances were quantitatively similar. The basis for the 'activation' of the Rb^+ conductance at −50 mV is unknown, but conceivably could involve the relief of K^+ (or some other ion) binding to a site within the channel that is accessible from the cytoplasmic side. To the extent that it reflects a change in single-channel conductance, the dramatic increase in macroscopic Kir7.1 conductance that occurs when external K^+ is replaced with Rb^+ suggests that the channel pore has a binding site with a higher affinity for K^+, as suggested by Wischmeyer *et al.* (2000). It remains to be determined, however, whether alterations in open probability or the number of functional channels might also be contributing factors.

The sole report of Kir7.1 single-channel conductance comes from the study of Krapivinsky *et al.* (1998), who applied non-stationary noise analysis to K^+ currents recorded from membrane patches of transfected mammalian cells to obtain an estimate of ∼50 fS. In the present study, we were unable to confirm these results in the *Xenopus* oocyte expression system. However, when we used Rb^+ as the permeant cation (together with Ba^{2+} to produce a time-dependent change in channel open probability), non-stationary noise analysis yielded a single-channel conductance of ∼2 pS. Assuming that channel gating and the number of functional channels are unaffected by Rb^+, our macroscopic conductance measurements would suggest a 10-fold smaller single-channel K^+ conductance of ∼200 fS. This value is ∼4 times larger than that estimated by Krapivinsky *et al.* (1998) but well within the accuracy of noise measurements. Thus, our results confirm that Kir7.1 has a very low single-channel conductance.

Kir7.1 channels comprise the RPE Kir conductance

It is well established that the membrane properties of isolated RPE cells are dominated by a mild, inwardly rectifying K^+ conductance (Hughes & Steinberg, 1990; Segawa & Hughes, 1994; Hughes, *et al.* 1995*b*; Hughes & Takahira, 1998) and there are several lines of evidence suggesting that this conductance lies in the apical membrane (Segawa & Hughes, 1994; Hughes *et al.* 1995*a*). In previous studies on amphibian (Hughes & Steinberg, 1990; Segawa & Hughes, 1994) and human RPE (Hughes & Takahira, 1996), we demonstrated that, in the vicinity of E_K, this conductance has the unusual property of decreasing in response to increases in $[K^+]_o$. In the present study on bovine RPE cells, we measured Kir conductance over a wider range of K^+ concentrations and confirmed this behaviour. Moreover, we extended these findings by examining the cation selectivity of the RPE Kir conductance and found that although it is nearly equally permeable to Rb^+ and K^+, it is 10 times more conductive to Rb^+ than to K^+. In addition, we estimate that the channel has a unitary Rb^+ conductance of ∼2 pS. These values are in close agreement with those obtained for the heterologously expressed Kir7.1 channel, strongly suggesting that Kir7.1 channel subunits comprise the Kir conductance of the RPE apical membrane. This conclusion is supported by the results of cell-attached recordings, which revealed inwardly rectifying Rb^+ currents mainly in apical membrane patches.

Although the Kir conductance in bovine RPE cells was qualitatively similar to the Kir7.1 conductance examined in oocytes, it differed in some respects. Compared to the cloned Kir7.1 conductance, the decrease in RPE Kir conductance produced by increasing $[K^+]_o$ was less pronounced. Moreover, in RPE cells bathed with low $[K^+]$, outward Kir currents were relatively smaller and exhibited less inactivation at positive potentials. The reason for these discrepancies is unknown, but one possibility is that the RPE and oocyte differ with respect to the intracellular concentrations of cytoplasmic blockers such as Mg^{2+} and polyamines, which are known to affect outward currents through other Kir channel types. Alternatively, there may be differences in post-translational modification of the channel subunit protein. Whole-cell recordings of Kir7.1 channels expressed in mammalian cells may help resolve this issue.

Recently, Kusaka *et al.* (1999) presented immunohistochemical and single-channel current data suggesting that Kir4.1 channels are present in the apical processes of neonatal rat RPE. Kir4.1 channels are characterized by moderate inward rectification, a strong dependence of macroscopic conductance on extracellular $[K^+]$, high sensitivity to block by Cs^+ and Ba^{2+}, inactivation at strong negative potentials and a single-channel K^+ conductance of 20–25 pS (Takumi *et al.* 1995). None of these properties, however, are shared by the predominant Kir conductance in amphibian (Hughes & Steinberg, 1990; Segawa & Hughes, 1994), human (Hughes *et al.* 1995*b*) or bovine RPE (Hughes & Takahira, 1998; this study). To reconcile this discrepancy, Kusaka *et al.* (1999) suggested that Kir.4.1 currents are not detected in whole-cell recordings because apical processes are lost from isolated RPE cells. In our experience, however, processes are generally present on the apical surface of isolated RPE cells (Hughes & Steinberg, 1990; Hughes *et al.* 1995*b*), and membrane capacitance measurements indicate that they are voltage clamped in whole-cell recordings. Hence, we conclude that if Kir4.1 channels are present in the RPE apical membrane, their contribution to the macroscopic conductance is minor compared to that of Kir7.1 channels.

Physiological significance

The RPE has an intimate anatomical and functional relationship with the adjacent photoreceptor cells. Microvilli projecting from the apical surface of the RPE interdigitate with the distal third of photoreceptor outer segments. Separating the RPE apical membrane and plasma membrane of the outer segment is a small extracellular compartment called the subretinal space. The RPE provides crucial support to the photoreceptors by regulating this microenvironment through the vectorial transport of fluid, ions and metabolites. K^+ channels in the apical membrane function directly in subretinal K^+ homeostasis by determining the direction and magnitude of net K^+ transport across the RPE (Miller & Edelman, 1990; Joseph & Miller, 1991). They also influence the net transport of HCO_3^- (Hughes *et al.* 1989) and Cl^- (Bialek & Miller, 1994) by affecting the electrochemical driving forces on these anions and also support Na^+–K^+ pump activity by providing a recycling pathway for K^+ across the apical membrane.

One of the unique features of the RPE is that, like the choroid plexus, the Na^+–K^+ pump is localized to the apical rather than the basolateral membrane (Steinberg & Miller, 1973; Okami *et al.* 1990), which is typical of most other transporting epithelia (Rodriguez-Boulan & Zurzolo, 1993). The results of our cell-attached recordings from isolated RPE cells indicate that channels with the hallmarks of Kir7.1 are also localized to the apical membrane. The capacity of the Kir7.1 channel to conduct relatively large outward currents makes it well suited to serve as the obligatory return pathway for K^+ that enters the cell through the Na^+–K^+ pump. On the basis of our meansurements of single-channel and whole-cell Rb^+ conductance, we estimate that there are $> 61\,000$ Kir7.1 channels in the apical membrane of each RPE cell. Assuming that these channels are distributed along the length of the microvilli, then their low unitary conductance and large number might serve to distribute the K^+ conductance and help minimize local K^+ gradients within the processes and extracellular space and thus optimize Na^+–K^+ pump function.

In addition to their function in transport processes, apical membrane K^+ channels also play an important role in RPE–photoreceptor interactions. At light onset, the closure of cGMP-gated cation channels in the photoreceptor outer segments leads to a decrease in subretinal $[K^+]$ from approximately 5 mM to 2 mM. By virtue of the presence of K^+ channels in the apical membrane, this $[K^+]_o$ decrease produces an apical membrane hyperpolarization, which generates the c-wave of the DC electroretinogram (Oakley & Green, 1976). At the same time, it triggers a large efflux of K^+ (and, secondarily, Cl^- and water) from the RPE, leading to reciprocal changes in the volumes of the RPE cell (Bialek & Miller, 1994) and subretinal space (Huang & Karwoski, 1992; Li *et al.* 1994).

One of the important features of the Kir channel in the RPE is that its macroscopic outward conductance increases with decreases in extracellular K^+ concentration (Segawa & Hughes, 1994; Hughes & Takahira, 1996). In the present study, we confirmed this finding in bovine RPE cells (Fig. 8) and show that it is an inherent property of the Kir7.1 channel (Fig. 3). This is opposite to the behaviour of other cloned and native Kir channels, which typically exhibit a decrease in outward (and inward) conductance with decreases in $[K^+]_o$ (Nichols & Lopatin, 1997). Our results suggest that, at light onset, an increase in the outward conductance of Kir7.1 channels might conspire with an increase in electrochemical driving force (Bialek & Miller, 1994) to promote K^+ efflux across the RPE apical membrane.

Ausubel, F. M., Brent, R., Kingston, R. E., Moore, D. D., Seidman, J. G., Smith, J. A. & Struhl, K. (1996). *Current Protocols in Molecular Biology*. John Wiley & Sons, New York.

Baumgartner, W., Isias, L. & Sigworth, F. J. (1999). Two-microelectrode voltage clamp of *Xenopus* oocytes: Voltage errors and compensation for local current flow. *Biophysical Journal* **77**, 1980–1991.

Bialek, S. & Miller, S. (1994). K^+ and Cl^- transport mechanisms in bovine pigment epithelium that could modulate subretinal space volume and composition. *Journal of Physiology* **475**, 53–67.

Chang, J., Milligan, S., Li, Y., Campochiaro, P. A., Hyde, D. & Zack, D. J. (1997). Mammalian homolog of *Drosophila* retinal degeneration B rescues the mutant phenotype in the fly. *Journal of Neuroscience* **17**, 5881–5890.

Chang, J. T., Esumi, N., Moore, K., Li, Y., Zhang, S., Chew, C., Goodman, B., Amir Rattner, A., Moody, S., Stetten, G., Campochiaro, P. A. & Zack, D. J. (1999). Cloning and characterization of a secreted frizzled-related protein that is expressed by the retinal pigment epithelium. *Human Molecular Genetics* **8**, 575–583.

Choe, H., Sackin, H. & Palmer, L. G. (1998). Permeation and gating of an inwardly rectifying potassium channel. Evidence for a variable energy well. *Journal of General Physiology* **112**, 433–446.

Döring, F., Derst, C., Wischmeyer, E., Karschin, C., Schneggenburger, R., Daut, J. & Karschin, A. (1998). The epithelial inward rectifier channel Kir7.1 displays unusual K^+ permeation properties. *Journal of Neuroscience* **18**, 8625–8636.

Goldin, A. L. (1992). Maintenance of *Xenopus laevis* and oocyte injection. *Methods in Enzymology* **207**, 266–279.

Griff, E. R., Shirao, Y. & Steinberg, R. H. (1985). Ba^{2+} unmasks K^+ modulation of the Na^+-K^+ pump in the retinal pigment epithelium. *Journal of General Physiology* **86**, 853–876.

Hamill, O. P., Marty, A., Neher, E., Sakmann, B. & Sigworth, F. J. (1981). Improved patch-clamp techniques for high-resolution current recording from cells and cell-free membrane patches. *Pflügers Archiv* **391**, 85–100.

Heinemann, S. H. & Conti, F. (1992). Nonstationary noise analysis and application to patch clamp recordings. *Methods in Enzymology* **207**, 131–149.

Hille, B. (1992). *Ionic Channels of Excitable Membranes*, 2nd edn. Sinauer Associates Inc., Sunderland, MA, USA.

Ho, K., Nichols, C. G., Lederer, W. J., Lytton, J., Vassilev, P. M., Kanazirska, M. V. & Hebert, S. C. (1993). Cloning and expression of an inwardly rectifying ATP-regulated potassium channel. *Nature* **362**, 31–38.

Huang, B. & Karwoski, C. (1992). Light-evoked expansion of subretinal space volume in the retina of the frog. *Journal of Neuroscience* **12**, 4243–4252.

Hughes, B. A., Adorante, J. S., Miller, S. S. & Lin, H. (1989). Apical electrogenic $NaHCO_3$ cotransport. A mechanism for HCO_3 absorption across the retinal pigment epithelium. *Journal of General Physiology* **94**, 125–150.

Hughes, B. A., Gallemore, R. P. & Miller, S. S. (1998). Transport mechanisms in the retinal pigment epithelium. In *The Retinal Pigment Epithelium*: *Function and Disease*, ed. Marmor, M. F. & Wolfensberger, T. J., pp. 103–134. Oxford University Press, New York.

Hughes, B. A., Shaikh, A. & Ahmad, A. (1995*a*). Effects of Ba^{2+} and Cs^+ on apical membrane K^+ conductance in toad retinal pigment epithelium. *American Journal of Physiology* **268**, C1164–1172.

Hughes, B. A. & Steinberg, R. H. (1990). Voltage-dependent currents in isolated cells of the frog retinal pigment epithelium. *Journal of Physiology* **428**, 273–297.

Hughes, B. A. & Takahira, M. (1996). Inwardly rectifying K^+ currents in isolated human retinal pigment epithelial cells. *Investigative Ophthalmolology and Visual Science* **37**, 1125–1139.

Hughes, B. A. & Takahira, M. (1998). ATP-dependent regulation of inwardly rectifying K^+ current in bovine retinal pigment epithelial cells. *American Journal of Physiology* **275**, C1372–1383.

Hughes, B. A., Takahira, M. & Segawa, Y. (1995*b*). An outwardly rectifying K^+ current active near resting membrane potential in human retinal pigment epithelial cells. *American Journal of Physiology* **269**, 179–187.

Jackson, P. S. & Strange, K. (1996). Single channel properties of a volume sensitive anion channel: Lessons from noise analysis. *Kidney International* **49**, 1695–1699.

Joseph, D. P. & Miller, S. S. (1991). Apical and basement membrane ion transport mechanism in bovine retinal pigment epithelium. *Journal of Physiology* **435**, 439–463.

Kofuji, P., Davidson, N. & Lester, H. A. (1995). Evidence that neuronal G-protein-gated inwardly rectifying K^+ channels are activated by G beta gamma subunits and function as heteromultimers. *Proceeding of the National Academy of Sciences of the USA* **92**, 6542–6546.

Krapivinsky, G., Medina, I., Eng, L., Krapivinsky, L., Yang, Y. & Clapham, D. E. (1998). A novel inward rectifier K^+ channel with unique pore properties. *Neuron* **20**, 995–1005.

Kubo, Y., Baldwin, T. J., Jan, Y. N. & Jan, L. Y. (1993). Primary structure and functional expression of a mouse inward rectifier potassium channel. *Nature* **362**, 127–133.

Kusaka, S., Horio, Y., Fujita, A., Matsushita, K., Inanobe, A., Gotow, T., Uchiyama, Y., Tano, Y. & Kurachi, Y. (1999). Expression and polarized distribution of an inwardly rectifying K^+ channel, Kir4.1, in rat retinal pigment epithelium. *Journal of Physiology* **520**, 373–381.

Lasansky, A. & De Fisch, F. W. (1966). Potential, current, and ionic influxes across the isolated retinal pigment epithelium and choroid. *Journal of General Physiology* **49**, 913–924.

Li, J. D., Gallemore, R. P., Dmitriev, A. & Steinberg, R. H. (1994). Light-dependent hydration of the space surrounding the photoreceptors in chick retina. *Investigative Ophthalmology and Visual Science* **35**, 2700–2711.

Löffler, K. & Hunter, M. (1997). Cation permeation and blockade of ROMK1, a cloned renal potassium channel. *Pflügers Archiv* **434**, 151–158.

Lopatin, A. N. & Nicholas, C. G. (1996). $[K^+]$ dependence of open channel conductance in cloned inward rectifier potassium channels (IRK1, Kir2.1). *Biophysical Journal* **71**, 682–694.

Miller, S. S. & Edelman, J. L. (1990). Active ion transport pathways in the bovine retinal pigment epithelium. *Journal of Physiology* **424**, 283–300.

Miller, S. S. & Steinberg, R. H. (1977). Passive ionic properties of frog retinal pigment epithelium. *Journal of Membrane Biology* **36**, 337–372.

Miller, S. S., Steinberg, R. H. & Oakley, B. I. (1978). The electrogenic sodium pump of the frog retinal pigment epithelium. *Journal of Membrane Biology* **67**, 199–209.

Nakamura, N., Suzuki, Y., Ikeda, Y., Notoya, M. & Hirose, S. (2000). Complete structure and regulation of the rate gene for inward rectifier potassium channel Kir7.1. *Journal of Biological Chemistry* **275**, 28276–28284.

Nakamura, N., Suzuki, Y., Sakuta, H., Ookata, K., Kawahara, K. & Hirose, S. (1999). Inwardly rectifying K^+ channel Kir7.1 is highly expressed in thyroid follicular cells, intestinal epithelial cells and choroid plexus epithelial: implication for a functional coupling with Na^+,K^+-ATPase. *Biochemical Journal* **342**, 329–336.

Nichols, C. G. & Lopatin, A. N. (1997). Inward rectifier potassium channel. *Annual Review of Physiology* **59**, 171–191.

Oakley, B. I. & Green, D. G. (1976). Correlation of light-induced changes in retinal extracellular potassium concentration with c-wave of the electroretinogram. *Journal of Neurophysiology* **39**, 1117–1133.

Okami, T., Yamamoto, A., Omori, K., Takada, T., Uyama, M. & Tashiro, Y. (1990). Immunocytochemical localization of Na^+,K^+-ATPase in rat retinal pigment epithelial cells. *Journal of Histochemistry and Cytochemistry* **38**, 1267–1275.

Partiseti, M., Collura, V., Agnel, M., Culouscou, J. M. & Graham, D. (1998). Cloning and characterization of a novel human inwardly rectifying potassium channel predominantly expressed in small intestine. *FEBS Letters* **434**, 171–176.

Quinn, R. H. & Miller, S. S. (1992). Ion transport mechanisms in native human retinal pigment epithelium. *Investigative Ophthalmology and Visual Science* **33**, 3513–3527.

Reimann, F. & Ashcroft, F. M. (1999). Inwardly rectifying potassium channels. *Current Opinion in Cell Biology* **11**, 503–508.

Reuveny, E., Jan, Y. N. & Jan, L. Y. (1996). Contributions of a negatively charged residue in the hydrophobic domain of the IRK1 inwardly rectifying K^+ channel to K^+-selective permeation. *Biophysical Journal* **70**, 754–761.

Rodriguez-Boulan, E. & Zurzolo, C. (1993). Polarity signals in epithelial cells. *Journal of Cell Science Supplement* **17**, 335–343.

Sambrook, J., Fritsch, F. F. & Maniatis, T. (1989). *Molecular Cloning, a Laboratory Manual*. Cold Spring Harbor Laboratory Press, New York.

Segawa, Y. & Hughes, B. A. (1994). Properties of the inwardly rectifying K^+ conductance in the toad retinal pigment epithelium. *Journal of Physiology* **476**, 41–53.

Shimura, M., Yuan, Y. & Hughes, B. A. (1999). Cation permeability of the inwardly rectifying potassium conductance in bovine retinal pigment epithelial (RPE) cells. *Investigative Ophthalmology and Visual Science* **40**, S499 (abstract).

Shuck, M. E., Piser, T. M., Bock, J. H., Slightom, J. L., Lee, K. S. & Bienkowski, M. J. (1997). Cloning and characterization of two K^+ inward rectifier (Kir) 1.1 potassium channel homologs from human kidney (Kir1.2 and Kir1.3). *Journal of Biological Chemistry* **272**, 586–593.

Standen, N. B. & Stanfield, P. R. (1980). Rubidium block and rubidium permeability of the inward rectifier of frog skeletal muscle fibers. *Journal of Physiology* **304**, 415–435.

Steinberg, R. & Miller, S. (1973). Aspects of electrolyte transport in frog pigment epithelium. *Experimental Eye Research* **16**, 365–372.

Stuhmer, W. (1992). Electrophysiological recording from *Xenopus* oocytes. *Methods in Enzymology* **207**, 319–339.

Takahira, M. & Hughes, B. A. (1997). Isolated bovine retinal pigment epithelial cells express delayed rectifier type and M-type K^+ currents. *American Journal of Physiology* **273**, C790–803.

Takumi, T., Ishii, T., Horio, Y., Morishige, K., Takahashi, N., Yamada, M., Yamashita, T., Kiyama, H., Sohmiya, K., Nakanishi, S. & Kurachi, Y. (1995). A novel ATP-dependent inward rectifier potassium channel expressed predominantly in glial cells. *Journal of Biological Chemistry* **270**, 16339–16346.

Traynelis, S. F. & Jaramillo, F. (1998). Getting the most out of noise in the central nervous system. *Trends in Neurosciences* **21**, 137–145.

Welling, P. A. (1997). Primary structure and functional expression of a cortical collecting duct Kir channel. *American Journal of Physiology* **273**, F825–836.

Wischmeyer, E., Doring, F. & Karschin, A. (2000). Stable cation coordination at a single outer pore residue defines permeation properties in Kir channels. *FEBS Letters* **466**, 115–120.

Yuan, Y., Chang, J. T., Shimura, M., Campochiaro, P. A., Zack, D. J. & Hughes, B. A. (2000). Molecular cloning and functional expression of Kir7.1, an inwardly rectifying K^+ channel from the retinal pigment epithelium (RPE). *Investigative Ophthalmology and Visual Science* **41**, S613 (*abstract*).

Zhou, H., Tate, S. S. & Palmer, L. G. (1994). Primary structure and functional properties of an epithelial K channel. *American Journal of Physiology* **266**, C809–824.

Acknowledgements

We thank Anuradha Swaminathan and Drs Gyanendra Kumar, Yasunori Segawa and Masayuki Takahira for their assistance with certain aspects of this study and Dr Alan Goldin (University of California, San Diego) for kindly providing the pBSTA plasmid. This work waas supported by National Eye Institute Grants EYO8850 (B.A.H.), EYO7703 and P30EY1765, Foundation Fighting Blindness, Macular Vision and Steinbach Foundations and unrestricted funds from Research to Prevent Blindness, Inc. (R.P.B.). D.J.Z. is a recipient of a Career Development Award from RPB and M.S. a recipient of an award from the Naito Foundation.

Corresponding author

B. A. Hughes: W. K. Kellogg Eye Center, Department of Ophthalmology and Visual Sciences, University of Michigan, 1000 Wall Street, Ann Arbor, MI 48105, USA.

Email: bhughes@umich.edu